SIMULATIONS OF TWO TYPES OF ENERGETIC PARTICLE DRIVEN GEODESIC ACOUSTIC MODES AND THE ENERGY CHANNELING IN THE LARGE HELICAL DEVICE PLASMAS

H. WANG, Y. TODO, M. OSAKABE, T. IDO, Y. SUZUKI
National Institute for Fusion Science, National Institutes of Natural Science
Toki, Japan
Email: wanghao@nifs.ac.jp

Abstract

Energetic particle driven geodesic acoustic modes (EGAMs) in the Large Helical Device (LHD) plasmas are investigated using MEGA code. MEGA is a hybrid simulation code for energetic particles (EPs) interacting with a magnetohydrodynamic (MHD) fluid. In the present work, both the conventional and extended models of MEGA are employed. In the conventional model, only the EPs are described by the kinetic equations, while in the extended model not only the EPs but also the thermal ions are described by them. Using MEGA with a conventional model, it is found that the transition between low frequency EGAM and high frequency EGAM is decided by the slope of EP velocity distribution. Also, the phase difference between the bulk pressure perturbation δP_{bulk} and EP pressure perturbation δP_{EP} are analysed. For the low frequency EGAMs, δP_{bulk} and δP_{EP} are in anti-phase. They cancel each other out, which reduces the restoring force of the oscillation leading to the low frequency. While for the high frequency EGAMs, δP_{bulk} and δP_{EP} are in the same phase. They enhance each other, and thus the frequencies are higher. Using MEGA with an extended model, the low frequency EGAMs are reproduced. Also, the energy transfer is analysed and the bulk ion heating during the EGAM activity is observed. The ions obtain energy when the EPs lose energy, and this indicates that an energy channel is established by EGAM. The EGAM channelling is reproduced by simulation for the first time. The heating power of bulk ions is 3.4 kW/m^3 which is close to the value 4 kW/m^3 evaluated from the experiments. It is found that the sideband resonance is dominant during the energy transfer from EGAM to the bulk ions, and the transit frequencies of resonant bulk ions are half EGAM frequency.

1. INTRODUCTION

Geodesic acoustic mode (GAM) is an oscillatory zonal flow coupled with density and pressure perturbations in toroidal plasmas[1-2]. In the past years, energetic particle driven GAM (EGAM) has been observed in JET, DIII-D, Large Helical Device (LHD), ASDEX-Upgrade, and HL-2A[3-9]. In the DIII-D experiment, the drops in neutron emission during the EGAM bursts suggest beam ion losses[4]. Also, in the LHD experiment, anomalous bulk ion heating during the EGAM activity suggests an energy channel created by EGAM[5]. In addition, EGAMs interact with turbulence and affect the plasma confinement[10-11]. Then, the understanding of the EGAMs is important for magnetic confinement fusion, because the energetic particles (EPs) need to be well confined and the bulk plasma heating needs to be improved.

Both the low-frequency and high-frequency branches of EGAM were predicted by Fu[12]. In addition, theory and simulation studies have been made to investigate the properties of low-frequency or high-frequency branch of EGAMs. These studies covered mode number, mode profile, mode excitation condition, and mode growth rate, etc., but only a few of them focused on the transition between the two branches. In order to extend the research of the frequency transition, the present proceeding investigates the transition between the two branches based on various EP distribution functions.

Not only the transition between the two EGAM branches, but also the mechanism of EGAM channelling, has not yet been deeply investigated by simulation, although the latter has direct significance for plasma heating efficiency. At present, the existence of EGAM energy channel has not been demonstrated by simulation. Also, it is quite conceivable that the bulk ions obtain energy from EGAM via Landau damping, but it is not clear which resonant bulk ions are the dominant. The present proceeding solves the above problems and gives clear evidence in the following sections.

2. SIMULATION MODEL AND PARAMETERS

A hybrid simulation code for EPs interacting with a magnetohydrodynamic (MHD) fluid, MEGA[13-15], is used for the simulation of EGAM. MEGA mainly includes two versions. In the conventional version, only the EPs are described by the kinetic equations, while in the extended version not only the EPs but also the thermal ions are described by them.

The simulation of the transition between two EGAM branches is conducted with the conventional version, and the simulation model is the same as Ref.[16]. In the conventional model, the bulk plasma is described by the nonlinear MHD equations. The drift kinetic description and the δf particle method are applied to the EPs. The EP contribution is included in the MHD momentum equation as the EP current density.

In the experiment of LHD, EGAM is excited in less than 1 s after the neutral beam injection, while the slowing down time in the discharge can be up to 10 s. This means that the EPs have not slowed down sufficiently and the distribution is a bump-on-tail type. A constant slowing-down time is assumed, and the charge exchange loss is considered for the simulation. In the case of very high charge exchange loss rate, the distribution function is close to the type of delta function; while in the case of extremely low charge exchange loss rate, the distribution function becomes a typical slowing-down type. Based on the above physical picture, the velocity distribution function f(v) is written as:

$$f(v) = C(v^3 + v_c^3)^{\frac{\tau_s}{3\tau_{cx}}-1} \quad , \tag{1}$$

where C is an integration constant, v_c is the critical velocity, τ_s is slowing down time which equals to 9.6 s, and τ_{cx} is charge exchange loss time. The shape of the distribution function is controlled by τ_s/τ_{cx}. For $\tau_{cx} \rightarrow \infty$, τ_s/τ_{cx} is 0 and the function is the typical slowing-down type, as shown by the dotted curve in Fig. 1(a). With increase of τ_s/τ_{cx}, more EPs distribute in the high-energy region and form a distribution with positive gradient in total velocity, as shown by the dashed curve in Fig. 1(a). Finally, with large τ_s/τ_{cx}, a typical bump-on-tail distribution is formed as shown by the solid curve in Fig. 1(a). The solid curve is a fit to the neutral particle analyser (NPA) measurement in LHD[5-6].
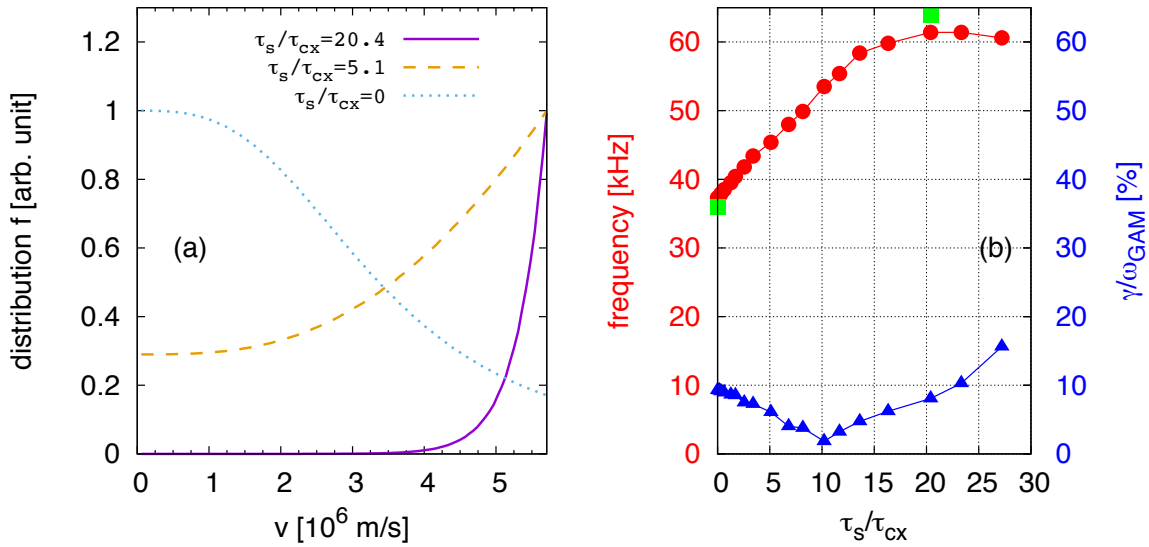

FIG. 1. (a) Slowing-down distribution without charge exchange loss represented by dotted line (τs/τcx =0) and bump-on-tail distribution with τs/τcx =20.4 represented by solid line. The dashed line represents a distribution in between. (b) The τs/τcx dependence of EGAM frequency and growth rate. Left vertical axis and circles represent frequencies in simulation, and the squares represent frequencies in experiment[6]. Right vertical axis and triangles represent growth rates.

The simulation of the EGAM channelling is conducted with the extended version, and the simulation model is the same as Ref. [15]. In the extended model, both the bulk ions and EPs are described kinetically. The following equations in the extended model are different from that in the conventional model:

$$\frac{\partial}{\partial t}(\rho \mathbf{u_{E\perp}}) = -\nabla(M\mathbf{u_{E\perp}}) - \nabla p_e + (\mathbf{j} - \frac{Z_i e}{m_i}\rho_i \mathbf{v_{pi}} - \frac{Z_h e}{m_h}\rho_h \mathbf{v_{ph}}) \times \mathbf{B} \tag{2}$$

$$\mathbf{E} = -\mathbf{u_{E\perp}} \times \mathbf{B} + \frac{\nabla_{\parallel}p_e}{(-e)n_e} + \eta(\mathbf{j} - \mathbf{j_{eq}}) \tag{3}$$

$$\rho = \rho_i + \rho_h \tag{4}$$

$$\mathbf{M} = \rho \mathbf{u_{E\perp}} + (\rho_i v_{i\parallel} + \rho_h v_{h\parallel})\mathbf{b} + \rho_i \mathbf{v_{pi}} + \rho_h \mathbf{v_{ph}} \qquad (5)$$

$$\rho_i \mathbf{v_{pi}} = \frac{m_i}{z_i e}\left(-\frac{\nabla p_{i\perp} \times \mathbf{B}}{B^2} + (p_{i\parallel} - p_{i\perp})\frac{\nabla \times \mathbf{b}}{B}\right) \qquad (6)$$

The Eq. (2) is momentum equation, and Eq. (3) is Ohm's law. The particle-in-cell (PIC) method is applied for ρ_i, ρ_h, $\rho_i v_{i\parallel}$, $\rho_h v_{h\parallel}$, $p_{i\parallel}$, $p_{i\perp}$, $p_{h\parallel}$, and $p_{h\perp}$.

A realistic 3-dimensional equilibrium generated by HINT code is used for the simulation[17]. This equilibrium data is based on the LHD shot #109031 at time t = 4.94 s. At this moment, the EGAM activity is very strong, thus it is good to reproduce the EGAM phenomenon. The parameters for the EGAM simulation are based on an LHD experiment[5-6]. The injected neutral beam energy is E_{NBI} = 170 keV. For simplicity, a slowing-down EP distribution is assumed in the proceeding. The bulk ion distribution is considered as Maxwellian.

3. SIMULATION OF THE TRANSITION BETWEEN TWO EGAM BRANCHES

The τ_s/τ_{cx} dependence of EGAM frequency and growth rate is investigated and shown in Fig. 1(b). From left to right, the slope of EP velocity distribution changes from negative to positive. The EGAM frequency increases with the increasing of τ_s/τ_{cx}. In other words, the EGAM frequency is decided by the slope of EP velocity distribution. This is easy to understand. For smaller τ_s/τ_{cx}, the EP distribution is more like a slowing-down type, and more EPs have relatively lower velocities and lower transit frequencies, and thus, the excited EGAM has lower frequency. For larger τ_s/τ_{cx}, the situation is opposite, and thus the excited EGAM has higher frequency. The two squares represent frequencies in experiment[5-6], and they are very close to the circles. This suggests that the simulated EGAM frequencies are consistent with the experiment observation. The EGAM growth rate is not a monotonic function of τ_s/τ_{cx}. With the increasing of τ_s/τ_{cx}, the growth rate firstly decreases, then increases. For the τ_s/τ_{cx} values between 5 and 15, the growth rates are very low and the modes are almost stable. This region can be considered as a transition region between low-frequency and high-frequency branches of EGAM, and this transition region can be explained by the slope of EP velocity distribution function. In the transition region, the slope of EP velocity distribution function is very close to 0, and thus, the drive from EPs become very weak and the mode growth rate become very low.

Both the low-frequency and high-frequency branches of EGAM have the same mode numbers and similar global mode structures, and then a question arises regarding why the two branches have different frequencies. EGAM is a kind of acoustic mode, and acoustic wave speed is decided by the pressure perturbation. Correspondingly, it can be speculated that the EGAM frequency is also decided by the pressure perturbation. In order to confirm this speculation, both the bulk pressure perturbation δP_{bulk} and EP pressure perturbation $\delta P_{EP\parallel}$ are analysed, as shown in Fig. 2. The most dominant component of pressure perturbation of EGAM is m/n = 1/0 sine. For simplicity, only this dominant component 1/0 sine is shown in figure. For the low-frequency branch, as shown in Fig. 2(a), the phase difference between δP_{bulk} and $\delta P_{EP\parallel}$ is π. The physical meaning is that they are in anti-phase and they cancel each other out. Thus, the frequency of the low-frequency branch of EGAM is low. For the high-frequency branch of EGAM, as shown in Fig. 2(b), the phases of δP_{bulk} and $\delta P_{EP\parallel}$ are the same, and they enhance each other. The high-frequency branch is driven by both δP_{bulk} and $\delta P_{EP\parallel}$. Thus, the frequency of the high-frequency branch of EGAM is high. From Fig. 2, it can be concluded that the EGAM frequency is indeed decided by the phase relation between δP_{bulk} and $\delta P_{EP\parallel}$. This conclusion is very similar to that in Ref. [18], although in Ref. [18] only the nonlinear properties were analysed but the linear frequency was not discussed. Until now, the phase relation of EGAMs in transition region has not been revealed, thus, Fig. 2(c) is plotted to show a transition case that τ_s/τ_{cx} = 5.1. It is found that the $\delta P_{EP\parallel}$ is very noisy, and thus, the phase relation is not able to be analysed. In fact, with the increasing of τ_s/τ_{cx}, the noise level of $\delta P_{EP\parallel}$ is not monotonic. The data firstly becomes more and more noisy, then becomes more and more clear.
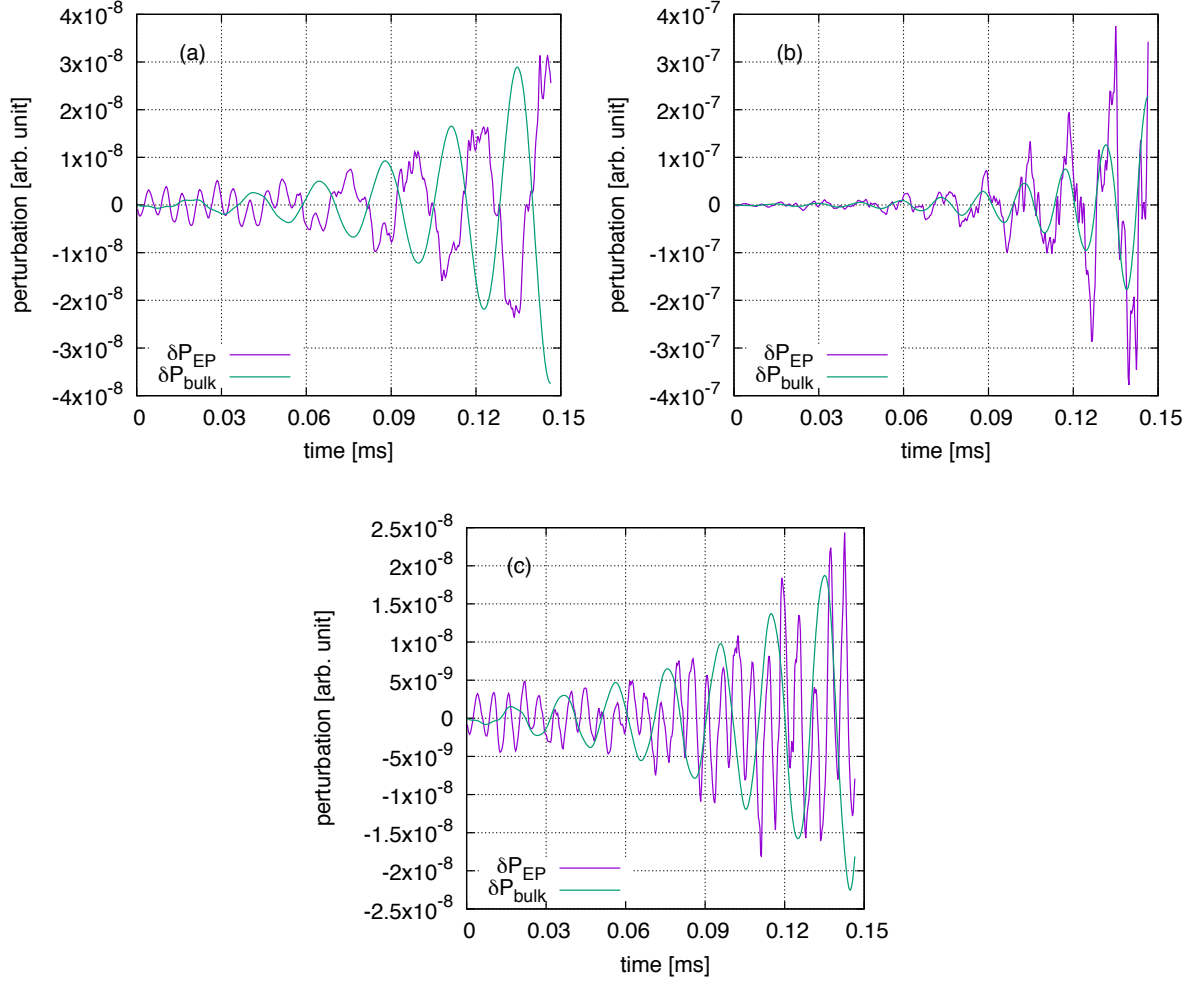
FIG. 2. The δP_bulk oscillation and the δP_EP|| oscillation of (a) low-frequency branch of EGAM, (b) high-frequency branch of EGAM, and (c) the EGAM in the transition region.

4.   SIMULATION OF EGAM CHANNELING

The extended model of MEGA code was applied to the LHD experiment. Figure 3(a) shows the spatial profile of the simulated mode. This mode peaks around r/a = 0.2, the mode width is about 0.4a, and the mode structure is very similar to Fig. 4 of Ref. [12]. The simulated mode is identified as a global mode, which is consistent with the global structure of EGAM. The dominant mode number is m/n = 0/0 for poloidal velocity as represented by the red curve in Fig. 3(a). Also, the dominant mode number is m/n = 1/0 for pressure perturbation. These mode numbers are also consistent with the nature of EGAM. Finally, the magnetic perturbation is much weaker than the poloidal velocity perturbation, and this indicates that it is an electrostatic mode. This is also consistent with the nature of EGAM. Thus, based on the above 3 properties, the simulated global electrostatic mode is identified as an EGAM. This the first time to reproduce an EGAM using the extended model of MEGA code. In addition, the simulated EGAMs' linear frequencies are between 40 kHz to 50 kHz as shown in Fig. 3(b), lower than the theoretically predicted conventional GAM frequency 54 kHz, thus these are low frequency branches of EGAM. The mode frequency decreases with the increasing of EP pressure, and this is consistent with the EGAM property.
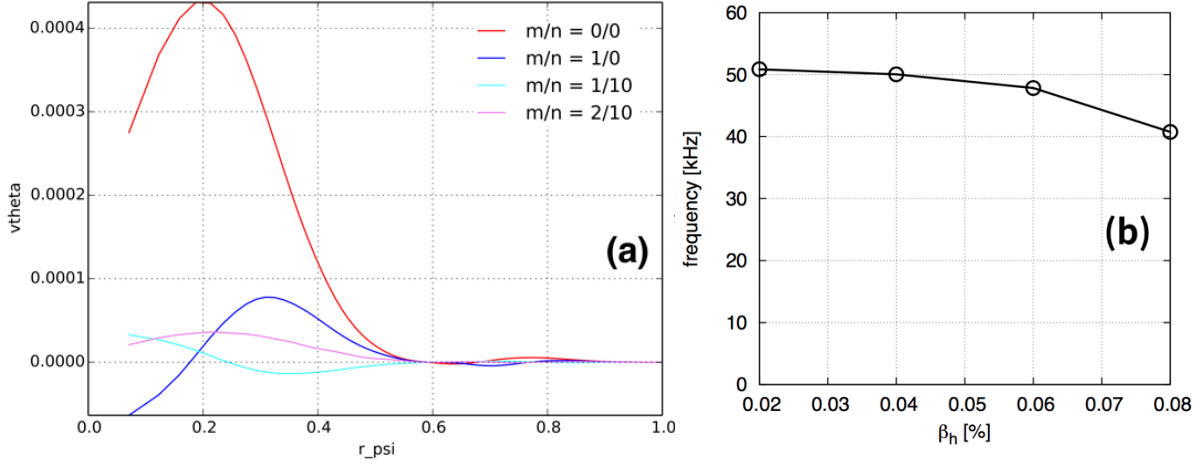
FIG. 3. (a) Poloidal velocity profile of the EGAM. (b) The EP pressure dependence of EGAM frequency in the linear growth phase.

A typical case is simulated to demonstrate the EGAM channelling phenomenon as shown in Fig. 4. Figure 4(a) shows the frequency spectrum of simulated EGAM. The mode frequency in linear stage is 50 kHz, and then, frequency chirps up in the nonlinear phase with time evolution. At t = 0.5 ms, the frequency has already exceeded 60 kHz. Fig. 4(b) shows the time evolution of EGAM amplitude v_θ. The linear stage is from t = 0 to about t = 0.1 ms. At t = 0.1 ms, the mode amplitude reaches the maximum value, and then, steps into the nonlinear phase. Fig. 4(c) shows the energy transfer of various species. The product of the perpendicular current of each species and the electric field is integrated in space and time. The perpendicular current consists of grad-B and curvature drift current, and magnetization current. The bulk ion heating during the EGAM activity is observed. The ions obtain energy when the EPs lose energy, and this indicates that an energy channel is established by EGAM. The EGAM channelling is reproduced by simulation for the first time. From t = 0 to t = 0.36 ms, the energy transferred from EP is 63 J. About half of this energy (51%) is transferred to bulk ions (34%) and electrons (17%), while another half is dissipated. The heating power of bulk ions around t = 0.1 ms is 3.4 kW/m^3 which is close to the value 4 kW/m^3 evaluated from the experiments[5].
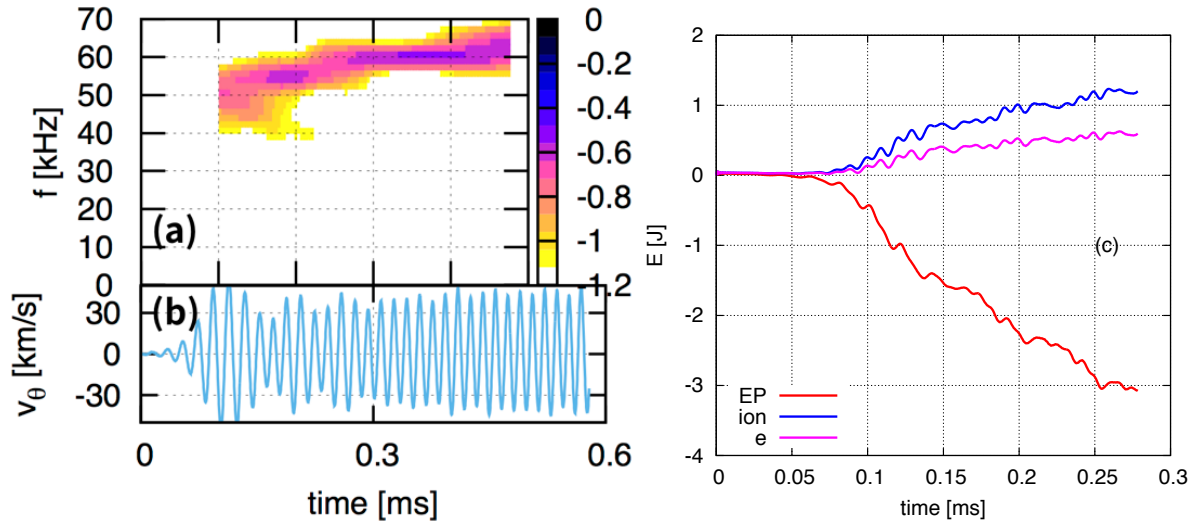

FIG. 4. (a) The frequency spectrum of EGAM. (b) The time evolution of EGAM amplitude v_θ. (c) Energy transfer of various species during EGAM activity.

In order to investigate the resonant particles, the δf distribution of both EPs and bulk ions at different times are analysed in the particle transit frequency space, as shown in Fig. 5. The particle transit frequency f_{tr} is defined by $f_{tr} = v_\parallel / (2\pi q R_0)$, where $v_\parallel$ is particle parallel velocity, q is the safety factor value, and $R_0 = 3.75$ m is plasma major radius. For simplicity of f_{tr} calculation, q = 2.8 is a constant for all the particles in the above f_{tr} equation, although q value has a normal shear profile in the equilibrium of simulation. The EGAM obtains energy from EPs via

5

inverse Landau damping, and EGAM transfer energy to bulk ions via Landau damping. These processes modify the distribution function of both EPs and bulk ions, and thus, δf values change with mode evolution. The negative δf value forms the hole structure in phase space, and the positive δf value forms the clump structure. Large absolute δf values indicate strong interactions between EGAM and resonant particles. Fig. 5(a) shows the resonant EPs. A hole around f_{tr} = 50 kHz is formed. The transit frequencies of particles in the hole increase with time evolution, and this increase of frequency is kept consistent with the chirping up of EGAM frequency. The resonance condition between EGAM and EPs is given by $f_{EGAM} = f_{tr,EP}$. Fig. 5(b) shows the resonant bulk ions. Two groups of clumps around f_{tr} = 25 kHz and f_{tr} = 5 kHz are formed. The transit frequencies of bulk ions in these clumps increase with time evolution, and these transit frequencies are kept at half the EGAM frequency (and one-tenth of EGAM frequency). The resonance condition between EGAM and bulk ions is given by

$$f_{EGAM} = l \cdot f_{tr,bulk} \quad , \qquad\qquad (7)$$

and dominant l values are l = 2 and l = 10. This is the first time to quantitatively reveal the resonance condition between EGAM and bulk ions during the establishment of EGAM channelling.
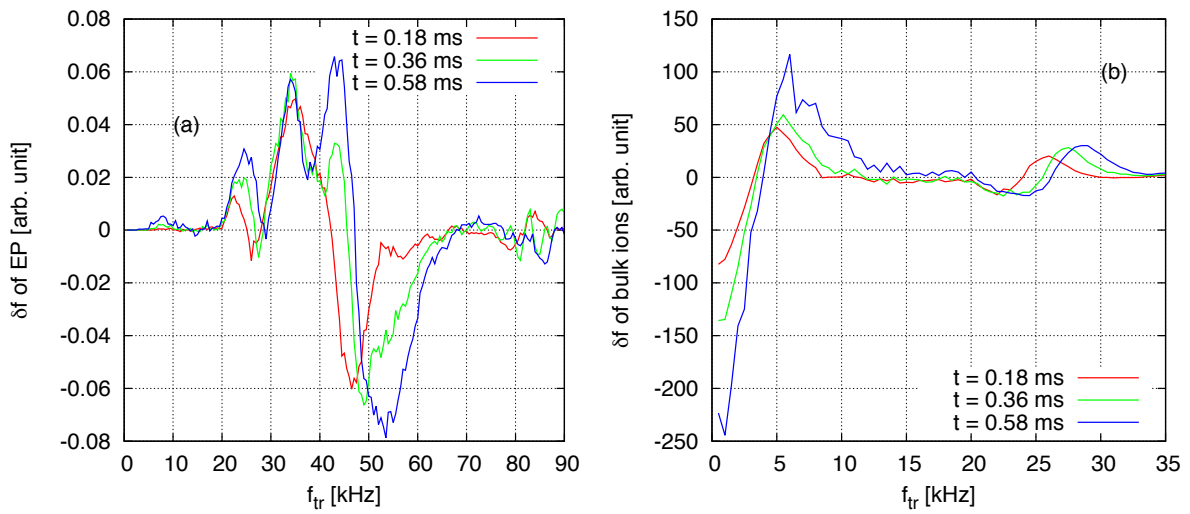

FIG. 5. The δf distribution of (a) EPs and (b) bulk ions in f_{tr} phase space at t = 0.18 ms (red), t = 0.36 ms (green), and t = 0.58 ms (blue).

In Eq. (7), l = 2 is important because l=2 sideband resonance condition is much easier to be satisfied than higher l value cases. However, l = 10 corresponds to very low transit frequency ions, and these low transit frequency ions should be difficult to obtain energy from EGAM. In order to confirm that, the energy transfer rate of bulk ions in f_{tr} phase space is analysed as shown in Fig. 6. There is a peak around f_{tr} = 25 kHz, and this peak gradually moves rightward. Similar to Fig. 5(b), this rightward moving indicates that the bulk ions with half mode frequency are kept resonant with the mode. The energy transfer rate is positive, and this indicates that the bulk ions absorb energy from EGAM. In Fig. 6, the red curve at t = 0.109 ms represents a transition between linear growth phase and nonlinear frequency chirping phase, this can also be confirmed from Fig. 4(b). From t = 0.145 ms in the fully nonlinear phase, another peak appears around f_{tr} = 15 kHz. In this simulation, the bulk ion temperature is 4.85 keV, and this thermal velocity corresponds to a transit frequency 14.7 kHz. The peak around f_{tr} = 15 kHz appears in Fig. 6 because most bulk ions' transit frequencies are around 15 kHz. In Fig. 5(b), there is a peak around 5 kHz, but this peak is very weak and difficult to identify in Fig. 6, because the particles around 5 kHz do not absorb too much energy. The bulk ions mainly absorb energy via the particles whose transit frequencies are half the EGAM frequency. In Eq. (7), l = 2 is more important than l = 10 for the establishment of EGAM channeling.
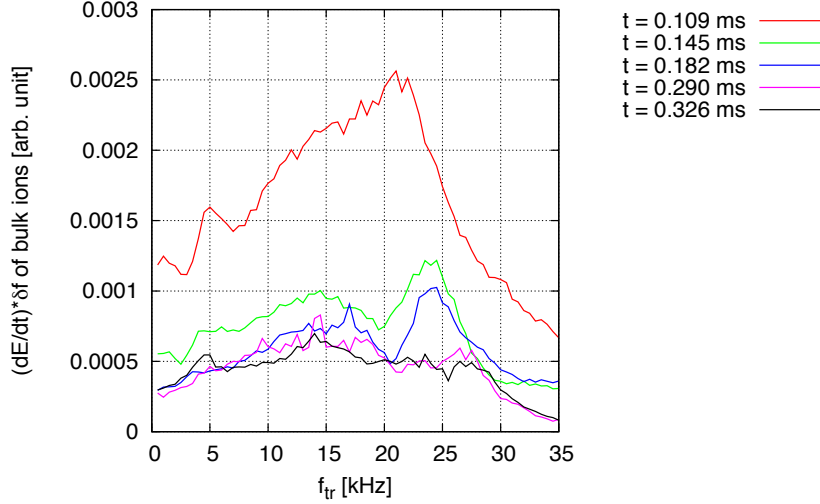
FIG. 6. Energy transfer rate of bulk ions in f_{tr} phase space at different times.

5.   SUMMARY AND CONCLUSIONS

In summary, both the transition between low-frequency and high-frequency branches of EGAM and EGAM channelling are investigated using MEGA code, and two different simulation models are applied respectively.

The transition between two branches of EGAM is simulated using the conventional model. In the case of slowing-down distribution, since more EPs have relatively lower velocities and lower transit frequencies, the low-frequency branch is excited. While in the case of bump-on-tail distribution, the situation is opposite, and thus the high-frequency branch is excited. In addition, the mechanism of frequency difference is clarified by the phase relation of bulk pressure perturbation δP_{bulk} and EP pressure perturbation $\delta P_{EP\parallel}$. For low-frequency branch, δP_{bulk} and $\delta P_{EP\parallel}$ are in anti-phase and they cancel each other out. While for high-frequency branch, the phases of δP_{bulk} and $\delta P_{EP\parallel}$ are the same. Thus, the frequencies of these 2 branches are different.

A global electrostatic mode is reproduced using extended model, and the mode is identified as an EGAM. Both the mode number and the mode frequency are consistent with the theoretical prediction. The ions obtain energy when the EPs lose energy during the EGAM activity, and this indicates that an energy channel is established by EGAM. The EGAM channelling is reproduced by simulation for the first time. The heating power of bulk ions is 3.4 kW/m³ which is close to the value 4 kW/m³ evaluated from the experiments[5]. The δf distribution of both EPs and bulk ions at different times are investigated, and the transit frequencies of resonant particles are analysed. Also, the energy transfer rate of bulk ions at different times are investigated and compared with δf distribution. The resonance condition $f_{EGAM} = l \cdot f_{tr,bulk}$ is satisfied where the dominant l values is l = 2. Another resonance with l=10 was also found. The resonance condition between EGAM and bulk ions during the establishment of EGAM channelling is quantitatively revealed for the first time.

REFERENCES

[1]   DIAMOND, P. et al., Zonal flows in plasma—a review, Plasma Phys. Control. Fusion **47** (2005) R35-R161.

[2] SUGAMA, H. and WATANABE, T., Collisionless damping of zonal flows in helical systems, Phys. Plasmas, **13** (2006) 012501.

[3] BOSWELL, C. et al., Observation and explanation of the JET n = 0 chirping mode, Phys. Lett. A **358** (2006) 154-158.

[4] NAZIKIAN, R. et al., Intense Geodesic Acousticlike Modes Driven by Suprathermal Ions in a Tokamak Plasma, Phys. Rev. Lett. **101** (2008) 185001.

[5] OSAKABE, M. et al., "Indication of bulk-ion heating by energetic particle driven Geodesic Acoustic Modes on LHD", Paper No. EX/10-3, IAEA Fusion Energy Conf., St. Pertersburg (2014).

[6] IDO, T. et al., Identification of the energetic-particle driven GAM in the LHD, Nucl. Fusion **55** (2015) 083024.

[7] IDO, T. et al., Strong Destabilization of Stable Modes with a Half-Frequency Associated with Chirping Geodesic Acoustic Modes in the Large Helical Device, Phys. Rev. Lett. **116** (2017) 015002.

[8] HORVATH, L. et al., Experimental investigation of the radial structure of energetic particle driven modes, Nucl. Fusion **56** (2016) 112003.

[9] CHEN, W. et al., Observation of energetic-particle-induced GAM and nonlinear interactions between EGAM, BAEs and tearing modes on the HL-2A tokamak, Nucl. Fusion **53** (2013) 113010.

[10] ZARZOSO, D. et al., Impact of Energetic-Particle-Driven Geodesic Acoustic Modes on Turbulence, Phys. Rev. Lett. **110** (2013) 125002.

[11] SASAKI, M. et al., Enhancement and suppression of turbulence by energetic-particle-driven geodesic acoustic modes, Scientific Reports, **7** (2017) 16767.

[12] FU, G. Y., Energetic-Particle-Induced Geodesic Acoustic Mode, Phys. Rev. Lett. **101** (2008) 185002.

[13] TODO, Y., Properties of energetic-particle continuum modes destabilized by energetic ions with beam-like velocity distributions, Phys. Plasmas, **13** (2006) 082503.

[14] TODO, Y. et al., Comprehensive magnetohydrodynamic hybrid simulations of fast ion driven instabilities in a Large Helical Device experiment, Phys. Plasmas, **24** (2017) 081203.

[15] TODO, Y., "A new magnetohydrodynamic hybrid simulation model with thermal and energetic ions", Paper No. O9, Int. Toki Conf. and Asia Plasma Fusion Association Conf., Toki (2017).

[16] WANG, H. et al., Simulation study of high-frequency energetic particle driven geodesic acoustic mode, Phys. Plasmas **22** (2015) 092507.

[17] SUZUKI, Y. et al., Development and application of HINT2 to helical system plasmas, Nucl. Fusion, **46** (2006) L19-L24.

[18] WANG, H. et al., Chirping and Sudden Excitation of Energetic-Particle-Driven Geodesic Acoustic Modes in a Large Helical Device Experiment, Phys. Rev. Lett. **120** (2018) 175001.